Estimation of plasma and brain METH concentrations

Male C57BL/6J mice (9-wk-old) and $Tyr^{c\text{-}2J}/Tyr^{c\text{-}2J}$ mice (9-wk-old) were injected with METH (4 mg/kg, i.p.) or saline, and 2 h after METH injection, the concentrations of METH in plasma and brain samples were determined by high-performance liquid chromatography (HPLC), as described previously (38). Brain samples were homogenized with four equivalent volumes of water per wet weight, immediately before extraction. Then, 50 µl of plasma samples and homogenized tissue samples were vortexed with 350 µl of acetonitrile containing 0.5 µg/ml β-phenylethylamine (PEA) as an internal standard and 10 µl of 10% sodium hydroxide. After deproteinization by centrifugation at 12,000 *g* for 5 min, the upper acetonitrile-rich layer was collected and evaporated to dryness under a stream of nitrogen gas at 45°C. The dried residues were reconstituted with 100 µl of 10 mM sodium carbonate-sodium bicarbonate buffer (pH 9.0) and 100 µl of 2 mM dansyl-chloride. Finally, samples were prepared for HPLC by heating them to 45°C for 1 h in the dark to derive dansyl-METH and dansyl-PEA from METH and PEA, respectively. The HPLC system consisted of a SIL-10ADvp autoinjector, a LC-10ADvp pump, a CTO-10ADvp column oven and RF-$10A_{XL}$ fluorescence detector, manufactured by Shimazu (Kyoto, Japan). Chromatograms were processed by a C-R8A Chromatopac chromatogram analyzer and recorder (Shimazu). Chromatographic separations were performed on a Cosmosil 5C18 column (4.6×150 mm; Nacalai Tesque, Kyoto, Japan) at 40°C. A prefiltered and degassed mobile phase consisting of 1 mM imidazole (adjusted to pH 7.0 with HNO_3)-acetonitrile (33:66, v/v) was delivered to the column at a flow rate of 0.8 ml/min, and the eluate was monitored by fluorescence detector (Em: 580 nm, Ex: 475 nm).

Protein measurement

Protein concentration was determined by the Bio-Rad DC protein assay kit (Bio-Rad, Richmond, CA), based on the Lowry assay, using bovine serum albumin as a standard.

Statistical analysis

Results are presented as mean ± SEM. Statistical significance was determined by one-way or two-way ANOVA followed by post hoc Fisher's PLSD test. A *P* value less than 0.05 denoted the presence of a statistically significant difference.

RESULTS

METH-induced neurotoxicity and quinoprotein formation in CATH.a cells

METH exposure (1–4 mM) for 24 h dose-dependently induced cell death in CATH.a cells with increases in LDH release (IC_{50}: ~2 mM), as shown in Fig. 1*A*. Therefore, METH was used in the following experiments at a concentration of 2 mM for CATH.a cells. Levels of quinoprotein formation also increased in a dose-dependent manner with METH treatment for 24 h (Fig. 1*B*), coinciding with cell toxicity (Fig. 1*A*).

Effects of quinone reductase inducer on METH-induced neurotoxicity and quinone formation in CATH.a cells

To confirm the possible involvement of quinone species formed by DA auto-oxidation in METH-induced cell death, we examined whether induction of intracellular quinone reductase [NAD(P)H: quinone oxidereductase-1 (NQO-1)], known to protect against the toxic effects of quinone by catalyzing two-electron reduction of quinone to the redox-stable hydroquinone (39, 40), might attenuate METH toxicity. Up-regulation of NQO-1 was achieved by treating CATH.a cells with quinone reductase inducer, BHA, and confirmed by Western blot analysis (167% of control) (Fig. 3). Pretreatment with BHA (25–100 μM) for 6 h on CATH.a cells significantly and dose-dependently reduced METH (2 mM)-induced neurotoxicity (Fig. 2*A*). BHA pretreatment also dramatically blocked METH-induced elevation of quinoprotein levels in a dose-dependent manner (Fig. 2*B*), in parallel with the cell toxicity results (Fig. 2*A*).

Effects of BHA and METH on NQO-1 expression in CATH.a cells

As shown in Fig. 3, METH treatment for 24 h induced NQO-1 expression in CATH.a cells, and pretreatment with 50 μM BHA before METH exposure, which alone promotes NQO-1 expression, significantly suppressed METH-induced NQO-1 expression.

Effects of DA depletion on METH-induced quinone formation in CATH.a cells

To examine the effects of DA depletion on METH-induced quinoprotein formation, CATH.a cells were pretreated with 1 μM reserpine or 100 μM α-MT for 24 h and then cotreated with 2 mM METH. We confirmed DA depletion caused by treatment with reserpine or α-MT by HPLC analysis; the DA content in CATH.a cells was reduced to almost 30% of control cells (data not shown). As shown in Fig. 4, pretreatment with reserpine and α-MT significantly reduced the METH-induced elevation of quinoprotein.

Effect of tyrosinase inhibitor on METH-induced neurotoxicity in CATH.a cells

Because tyrosinase in the brain enzymatically and rapidly oxidizes excessive amounts of cytosolic DA to form melanin, we examined the effect of tyrosinase inhibitor PTU on METH-induced neurotoxicity by LDH assay. PTU (50–250 μM) significantly enhanced METH neurotoxicity in CATH.a cells in a dose-dependent manner (Fig. 5).

METH-induced neurotoxicity and quinoprotein formation in BALB/c mice

Repeated METH injections have been reported to cause dopaminergic terminal loss shown as reduction of DAT-positive signals in the striatum of animals (5, 41). In this study, we confirmed the reduction of DAT-positive signals in the striatum of BALB/c mice 1, 3, and 14 days after repeated METH injections (4 mg/kg×4, i.p. with 2-h intervals). Marked reduction of DAT signals was observed in the striatum 3 days after METH injections, in agreement with many reports (5, 41), starting at 1 day through to 14 days (Fig. 6*A*, *B*). Quinoprotein levels in the striatum were significantly increased 3 and 14 days after the repeated METH injections (Fig. 6*C*), coinciding with reduction of DAT signals (Fig. 6*A*, *B*).

Involvement of tyrosinase in METH injections-induced neurotoxicity and quinoprotein formation in the striatum of mice

Because quinone formation in METH-induced neurotoxicity was also demonstrated using METH-injected mice in the present report, we further examined the possible regulatory effect of tyrosinase in protecting DA neurons from METH injections-induced neurotoxicity using albino tyrosinase null C57BL/6J-$Tyr^{c\text{-}2J}$/$Tyr^{c\text{-}2J}$ and wild-type C57BL/6J mice. Repeated METH injections (4 mg/kg×4, i.p. with 2 h intervals) showed moderate reduction of the DAT signal in the striatum of wild-type C57BL/6J mice 3 days after the injections (30% reduction of control) (Fig. 7*A*, *B*), which was less than the reduction in BALB/c mice (70% reduction of control) (Fig. 6*A*, *B*). In contrast, severe reduction of DAT signals was observed in the striatum of tyrosinase null $Tyr^{c\text{-}2J}$/$Tyr^{c\text{-}2J}$ mice 3 days after the METH injection (almost 90% reduction of control) (Fig. 7*A*, *B*). Basal quinoprotein levels in the striatum of $Tyr^{c\text{-}2J}$/$Tyr^{c\text{-}2J}$ mice were higher than those of C57BL/6J mice. METH injections significantly increased quinoprotein levels in the striatum of both wild-type and tyrosinase null mice. On day 3 after the METH injections, levels of striatal quinoprotein in $Tyr^{c\text{-}2J}$/$Tyr^{c\text{-}2J}$ mice were much higher than those in C57BL/6J mice (Fig. 7*C*).

Plasma and brain METH concentrations in C57BL/6J and $Tyr^{c\text{-}2J}$/$Tyr^{c\text{-}2J}$ mice

METH concentrations in the plasma and brain after injection of METH in control C57BL/6J and $Tyr^{c\text{-}2J}$/$Tyr^{c\text{-}2J}$ mice are shown in Fig. 8*A* and *B*. There were no differences in plasma and brain METH concentrations in C57BL/6J and $Tyr^{c\text{-}2J}$/$Tyr^{c\text{-}2J}$ mice 2 h after a single METH (4 mg/kg, i.p.) injection. The brain distribution of METH is shown in Fig. 8*C*, given as brain/plasma ratio (K*p*) values. There were no differences in the brain distributions between wild-type and tyrosinase null mice.

DISCUSSION

Auto-oxidation of cytosolic-free DA and consequent generation of ROS have been reported to be involved in METH-induced neurotoxicity in dopaminergic neurons (5–7, 42). Recently, the neurotoxicity of DA quinone formation by auto-oxidation of DA has focused on dopaminergic neuron-specific oxidative stress (25, 26). DA quinones exert cytotoxicity by interacting with the sulfhydryl group of the amino acid cysteine on various bioactive molecules, resulting predominantly in the formation of 5-cysteinyl-DA (15, 19). Because the sulfhydryl group on cysteine is often found at the active site of functional proteins, covalent modification of cysteine residues by quinones to form 5-cysteinyl-catechols irreversibly alters or inhibits protein function. Indeed, DA quinone covalently binds to key molecules of DA neurons, tyrosine hydroxylase, and DA transporter, to consequently inactivate those molecules (17, 18).

In the present study, we demonstrated the involvement of DA quinone formation in METH-induced dopaminergic neurotoxicity in vitro and in vivo. METH treatment increased intracellular quinoprotein formation in dopaminergic cells, coinciding with neurotoxicity. We also determined whether the induction of intracellular quinone reductase, NQO-1, could protect against METH toxicity. Up-regulation of NQO-1 was achieved by treating cells with quinone reductase inducer, BHA, as reported previously (43, 44). The induction of NQO-1 by BHA treatment dramatically and dose-dependently blocked METH-induced cytotoxicity and quinoprotein formation. METH treatment induced intracellular NQO-1 expression, and this

induction of NQO-1 was significantly suppressed by BHA pretreatment before METH exposure. The induction of NQO-1 with METH treatment may be a complementary reaction against quinone generation by METH treatment. Preinduced intracellular NQO-1 by BHA pretreatment for 6 h could eliminate generated quinones with METH exposure, and consequently the complementary induction level of NQO-1 24 h after METH treatment might be less than that in the group treated with METH alone. Thus, our present findings confirm that DA quinone formation is involved in METH-induced dopaminergic neurotoxicity. Furthermore, to confirm that quinone formation originated from intracellular auto-oxidized DA, we determined the effects of intracellular DA depletion on METH-induced quinoprotein formation. Intracellular DA depletion with reserpine or α-MT treatment significantly prevented the elevation of quinoprotein formation induced by METH exposure. These findings suggested that the reduction of endogenous DA could attenuate quinone toxicity. In fact, there are several reports showing that α-MT prevents the toxic effects of METH (4, 45, 46). Our present study has provided evidence suggesting that endogenous free DA plays an important role in mediating METH-induced neuronal damage. In addition, it is also suggested that DA quinone formation by auto-oxidation of endogenous DA may be important not only in METH toxicity but in other dopaminergic neurodegeneration, as well. Recently, we showed that repeated levodopa administration elevated striatal quinoprotein levels specifically on the parkinsonian side, not on the control side, of hemi-parkinsonian mice (47). The marked elevation of cytotoxic quinone generation specifically in the parkinsonian striatum after repeated levodopa administration suggested that excess amount of cytosolic DA in damaged dopaminergic nerve terminals after levodopa treatment is easily oxidized to DA quinones. In contrast, there is an argument showing that the cytotoxicity of DA may be an artifact of cell culture (48). However, Choi et al. (49) recently showed that increases in intrinsic DA levels but not extrinsic DA produce elevation of quinone formation, which may lead to selective dopaminergic neuronal damage. Our present data, together with previous reports, indicate that DA quinone formation plays an important role in the neurodegeneration as a dopaminergic neuron-specific neurotoxic factor.

In the present study, BHA pretreatment at high doses almost completely blocked METH-induced quinone formation, but partially inhibited METH-induced cytotoxicity. These suggest that METH-induced neurotoxicity is caused by not only quinone formation generated from endogenous free DA but also other factors such as ROS, nitric oxide, and excitatory amino acids.

The melanin-synthetic enzyme tyrosinase in the brain may rapidly oxidize excess amounts of cytosolic DA, thereby preventing slowly progressive cell damage by auto-oxidation of DA (26). In our previous report, we demonstrated that tyrosinase inhibition and transfection of antisense tyrosinase cDNA markedly reduced cell viability, increased intracellular DA, and enhanced DA-induced cell death in CATH.a cells (50), suggesting that the dysfunction of tyrosinase produces cell death by increasing intracellular DA levels and the consequent gradual auto-oxidation of DA to generate toxic ROS and reactive quinones, including DA quinone. In the present study, we showed the protective effects of tyrosinase, which enzymatically oxidizes DA and DA quinone to form melanin, against METH-induced dopaminergic neurotoxicity in vitro and in vivo. In particular, the reduction of DAT in the striatum induced by the METH injection was markedly aggravated in the tyrosinase null mice, compared with that in the METH-injected wild-type C57BL/6J mice. Interestingly, the basal quinoprotein level in the striatum of tyrosinase null mice was higher than that of wild-type C57BL/6J mice, suggesting vulnerability in tyrosinase null mice. These major differences between tyrosinase null and wild-type mice were

not due to brain distribution of the injected METH. These results suggest that tyrosinase plays a protective role against METH-induced dopaminergic neurotoxicity in neuronal cells by regulating quinone formation.

In conclusion, we confirmed that DA quinone formation is involved in the METH-induced dopaminergic neurotoxicity in vitro and in vivo as a dopaminergic neuron-specific neurotoxic factor. In addition, we demonstrated that quinone formation-related molecules such as quinone reductase and tyrosinase protect against METH neurotoxicity to reduce intracellular free DA and DA quinone (Fig. 9). Enhancing activities of quinone formation-related molecules such as quinone reductase would be a novel approach to prevent METH-induced neurotoxicity.

ACKNOWLEDGMENTS

This work was supported in part by Grants-in-Aid for Young Scientists (B) and for Scientific Research (C) from the Japanese Ministry of Education, Culture, Sports, Science, and Technology, and by Health and Labor Sciences Research Grants for Research on Psychiatric and Neurological Diseases and Mental Health, for Specific Research, and for Research on Measures for Intractable Diseases from the Japanese Ministry of Health, Labor and Welfare.

REFERENCES

1. Hotchkiss, A. J., and Gibb, J. W. (1980) Long-term effects of multiple doses of methamphetamine on tryptophan hydroxylase and tyrosine hydroxylase activity in rat brain. *J. Pharmacol. Exp. Ther.* **214,** 257–262

2. Ricaurte, G. A., Schuster, C. R., and Seiden, L. S. (1980) Long-term effects of repeated methylamphetamine administration on dopamine and serotonin neurons in the rat brain: a regional study. *Brain Res.* **193,** 153–163

3. Wagner, G. C., Ricaurte, G. A., Seiden, L. S., Schuster, C. R., Miller, R. J., and Westley, J. (1980) Long-lasting depletions of striatal dopamine and loss of dopamine uptake sites following repeated administration of methamphetamine. *Brain Res.* **181,** 151–160

4. Axt, K. J., Commins, D. L., Vosmer, G., and Seiden, L. S. (1990) alpha-Methyl-p-tyrosine pretreatment partially prevents methamphetamine-induced endogenous neurotoxin formation. *Brain Res.* **515,** 269–276

5. Cadet, J. L., and Brannock, C. (1998) Free radicals and the pathobiology of brain dopamine systems. *Neurochem. Int.* **32,** 117–131

6. Cubells, J. F., Rayport, S., Rajendran, G., and Sulzer, D. (1994) Methamphetamine neurotoxicity involves vacuolation of endocytic organelles and dopamine-dependent intracellular oxidative stress. *J. Neurosci.* **14,** 2260–2271

7. Fumagalli, F., Gainetdinov, R. R., Wang, Y. M., Valenzano, K. J., Miller, G. W., and Caron, M. G. (1999) Increased methamphetamine neurotoxicity in heterozygous vesicular monoamine transporter 2 knock-out mice. *J. Neurosci.* **19,** 2424–2431

8. LaVoie, M. J., and Hastings, T. G. (1999) Dopamine quinone formation and protein modification associated with the striatal neurotoxicity of methamphetamine: evidence against a role for extracellular dopamine. *J. Neurosci.* **19,** 1484–1491

9. Liu, Y., and Edwards, R. H. (1997) The role of vesicular transport proteins in synaptic transmission and neural degeneration. *Annu. Rev. Neurosci.* **20,** 125–156

10. Marek, G. J., Vosmer, G., and Seiden, L. S. (1990) Dopamine uptake inhibitors block long-term neurotoxic effects of methamphetamine upon dopaminergic neurons. *Brain Res.* **513,** 274–279

11. Seiden, L. S., and Vosmer, G. (1984) Formation of 6-hydroxydopamine in caudate nucleus of the rat brain after a single large dose of methylamphetamine. *Pharmacol. Biochem. Behav.* **21,** 29–31

12. Uhl, G. R. (1998) Hypothesis: the role of dopaminergic transporters in selective vulnerability of cells in Parkinson's disease. *Ann. Neurol.* **43,** 555–560

13. Wrona, M. Z., Yang, Z., Zhang, F., and Dryhurst, G. (1997) Potential new insights into the molecular mechanisms of methamphetamine-induced neurodegeneration. *NIDA Res. Monogr.* **173,** 146–174

14. Yuan, J., Callahan, B. T., McCann, U. D., and Ricaurte, G. A. (2001) Evidence against an essential role of endogenous brain dopamine in methamphetamine-induced dopaminergic neurotoxicity. *J. Neurochem.* **77,** 1338–1347

15. Graham, D. G. (1978) Oxidative pathways for catecholamines in the genesis of neuromelanin and cytotoxic quinones. *Mol. Pharmacol.* **14,** 633–643

16. Tse, D. C., McCreery, R. L., and Adams, R. N. (1976) Potential oxidative pathways of brain catecholamines. *J. Med. Chem.* **19,** 37–40

17. Kuhn, D. M., Arthur, R. E., Jr., Thomas, D. M., and Elferink, L. A. (1999) Tyrosine hydroxylase is inactivated by catechol-quinones and converted to a redox-cycling quinoprotein: possible relevance to Parkinson's disease. *J. Neurochem.* **73,** 1309–1317

18. Whitehead, R. E., Ferrer, J. V., Javitch, J. A., and Justice, J. B. (2001) Reaction of oxidized dopamine with endogenous cysteine residues in the human dopamine transporter. *J. Neurochem.* **76,** 1242–1251

19. Fornstedt, B., Rosengren, E., and Carlsson, A. (1986) Occurrence and distribution of 5-S-cysteinyl derivatives of dopamine, dopa and dopac in the brains of eight mammalian species. *Neuropharmacology* **25,** 451–454

20. LaVoie, M. J., and Hastings, T. G. (1999) Peroxynitrite- and nitrite-induced oxidation of dopamine: implications for nitric oxide in dopaminergic cell loss. *J. Neurochem.* **73,** 2546–2554

21. Haque, M. E., Asanuma, M., Higashi, Y., Miyazaki, I., Tanaka, K., and Ogawa, N. (2003) Apoptosis-inducing neurotoxicity of dopamine and its metabolites via reactive quinone generation in neuroblastoma cells. *Biochim. Biophys. Acta* **1619,** 39–52

22. Haque, M. E., Asanuma, M., Higashi, Y., Miyazaki, I., Tanaka, K., and Ogawa, N. (2003) Overexpression of Cu-Zn superoxide dismutase protects neuroblastoma cells against dopamine cytotoxicity accompanied by increase in their glutathione level. *Neurosci. Res.* **47,** 31–37

23. Lai, C. T., and Yu, P. H. (1997) Dopamine- and L-β-3,4-dihydroxyphenylalanine hydrochloride (L-Dopa)-induced cytotoxicity towards catecholaminergic neuroblastoma SH-SY5Y cells. Effects of oxidative stress and antioxidative factors. *Biochem. Pharmacol.* **53,** 363–372

24. Offen, D., Ziv, I., Sternin, H., Melamed, E., and Hochman, A. (1996) Prevention of dopamine-induced cell death by thiol antioxidants: possible implications for treatment of Parkinson's disease. *Exp. Neurol.* **141,** 32–39

25. Asanuma, M., Miyazaki, I., Diaz-Corrales, F. J., and Ogawa, N. (2004) Quinone formation as dopaminergic neuron-specific oxidative stress in pathogenesis of sporadic Parkinson's disease and neurotoxin-induced parkinsonism. *Acta Med. Okayama* **58,** 221–233

26. Asanuma, M., Miyazaki, I., and Ogawa, N. (2003) Dopamine- or L-DOPA-induced neurotoxicity: the role of dopamine quinone formation and tyrosinase in a model of Parkinson's disease. *Neurotox. Res.* **5,** 165–176

27. Hearing, V. J., and Ekel, T. M. (1976) Mammalian tyrosinase. A comparison of tyrosine hydroxylation and melanin formation. *Biochem. J.* **157,** 549–557

28. Miranda, M., and Botti, D. (1983) Harding-passey mouse-melanoma tyrosinase inactivation by reaction products and activation by L-epinephrine. *Gen. Pharmacol.* **14,** 231–237

29. Miranda, M., Botti, D., Bonfigli, A., Ventura, T., and Arcadi, A. (1984) Tyrosinase-like activity in normal human substantia nigra. *Gen. Pharmacol.* **15,** 541–544

30. Tief, K., Hahne, M., Schmidt, A., and Beermann, F. (1996) Tyrosinase, the key enzyme in melanin synthesis, is expressed in murine brain. *Eur. J. Biochem.* **241,** 12–16

31. Tief, K., Schmidt, A., Aguzzi, A., and Beermann, F. (1996) Tyrosinase is a new marker for cell populations in the mouse neural tube. *Dev. Dyn.* **205,** 445–456

32. Tief, K., Schmidt, A., and Beermann, F. (1997) Regulation of the tyrosinase promoter in transgenic mice: expression of a tyrosinase-lacZ fusion gene in embryonic and adult brain. *Pigment Cell Res.* **10,** 153–157

33. Tief, K., Schmidt, A., and Beermann, F. (1998) New evidence for presence of tyrosinase in substantia nigra, forebrain and midbrain. *Brain Res. Mol. Brain Res.* **53,** 307–310

34. Xu, Y., Stokes, A. H., Freeman, W. M., Kumer, S. C., Vogt, B. A., and Vrana, K. E. (1997) Tyrosinase mRNA is expressed in human substantia nigra. *Brain Res. Mol. Brain Res.* **45,** 159–162

35. Miyazaki, I., Iwata-Ichikawa, E., Asanuma, M., Iida, M., and Ogawa, N. (1999) Bifemelane hydrochloride protects against cytotoxicity of hydrogen peroxide on cultured rat neuroblastoma cell line. *Neurochem. Res.* **24,** 857–860

36. Paz, M. A., Fluckiger, R., Boak, A., Kagan, H. M., and Gallop, P. M. (1991) Specific detection of quinoproteins by redox-cycling staining. *J. Biol. Chem.* **266,** 689–692

37. Asanuma, M., Nishibayashi, S., Kondo, Y., Iwata, E., Tsuda, M., and Ogawa, N. (1995) Effects of single cyclosporin A pretreatment on pentylenetetrazol-induced convulsion and on TRE-binding activity in the rat brain. *Brain Res. Mol. Brain Res.* **33,** 29–36

38. Kitaichi, K., Morishita, Y., Doi, Y., Ueyama, J., Matsushima, M., Zhao, Y. L., Takagi, K., and Hasegawa, T. (2003) Increased plasma concentration and brain penetration of methamphetamine in behaviorally sensitized rats. *Eur. J. Pharmacol.* **464,** 39–48

39. Cavelier, G., and Amzel, L. M. (2001) Mechanism of NAD(P)H:quinone reductase: Ab initio studies of reduced flavin. *Proteins* **43,** 420–432

40. Joseph, P., Long, D. J., II, Klein-Szanto, A. J., and Jaiswal, A. K. (2000) Role of NAD(P)H:quinone oxidoreductase 1 (DT diaphorase) in protection against quinone toxicity. *Biochem. Pharmacol.* **60,** 207–214

41. Asanuma, M., Tsuji, T., Miyazaki, I., Miyoshi, K., and Ogawa, N. (2003) Methamphetamine-induced neurotoxicity in mouse brain is attenuated by ketoprofen, a non-steroidal anti-inflammatory drug. *Neurosci. Lett.* **352,** 13–16

42. Kita, T., Wagner, G. C., and Nakashima, T. (2003) Current research on methamphetamine-induced neurotoxicity: animal models of monoamine disruption. *J. Pharmacol. Sci.* **92,** 178–195

43. Choi, H. J., Kim, S. W., Lee, S. Y., and Hwang, O. (2003) Dopamine-dependent cytotoxicity of tetrahydrobiopterin: a possible mechanism for selective neurodegeneration in Parkinson's disease. *J. Neurochem.* **86,** 143–152

44. Munday, R., Smith, B. L., and Munday, C. M. (1998) Effects of butylated hydroxyanisole and dicoumarol on the toxicity of menadione to rats. *Chem. Biol. Interact.* **108,** 155–170

45. Schmidt, C. J., Ritter, J. K., Sonsalla, P. K., Hanson, G. R., and Gibb, J. W. (1985) Role of dopamine in the neurotoxic effects of methamphetamine. *J. Pharmacol. Exp. Ther.* **233,** 539–544

46. Wagner, G. C., Lucot, J. B., Schuster, C. R., and Seiden, L. S. (1983) Alpha-methyltyrosine attenuates and reserpine increases methamphetamine-induced neuronal changes. *Brain Res.* **270,** 285–288

47. Miyazaki, I., Asanuma, M., Diaz-Corrales, F. J., Miyoshi, K., and Ogawa, N. (2005) Dopamine agonist pergolide prevents levodopa-induced quinoprotein formation in parkinsonian striatum and shows quenching effects on dopamine-semiquinone generated in vitro. *Clin. Neuropharmacol.* **28,** 155–160

48. Clement, M. V., Long, L. H., Ramalingam, J., and Halliwell, B. (2002) The cytotoxicity of dopamine may be an artefact of cell culture. *J. Neurochem.* **81,** 414–421

49. Choi, H. J., Lee, S. Y., Cho, Y., and Hwang, O. (2005) Inhibition of vesicular monoamine transporter enhances vulnerability of dopaminergic cells: relevance to Parkinson's disease. *Neurochem. Int.* **46,** 329–335

50. Higashi, Y., Asanuma, M., Miyazaki, I., and Ogawa, N. (2000) Inhibition of tyrosinase reduces cell viability in catecholaminergic neuronal cells. *J. Neurochem.* **75,** 1771–1774

Received September 2, 2005; accepted October 28, 2005

Fig. 1

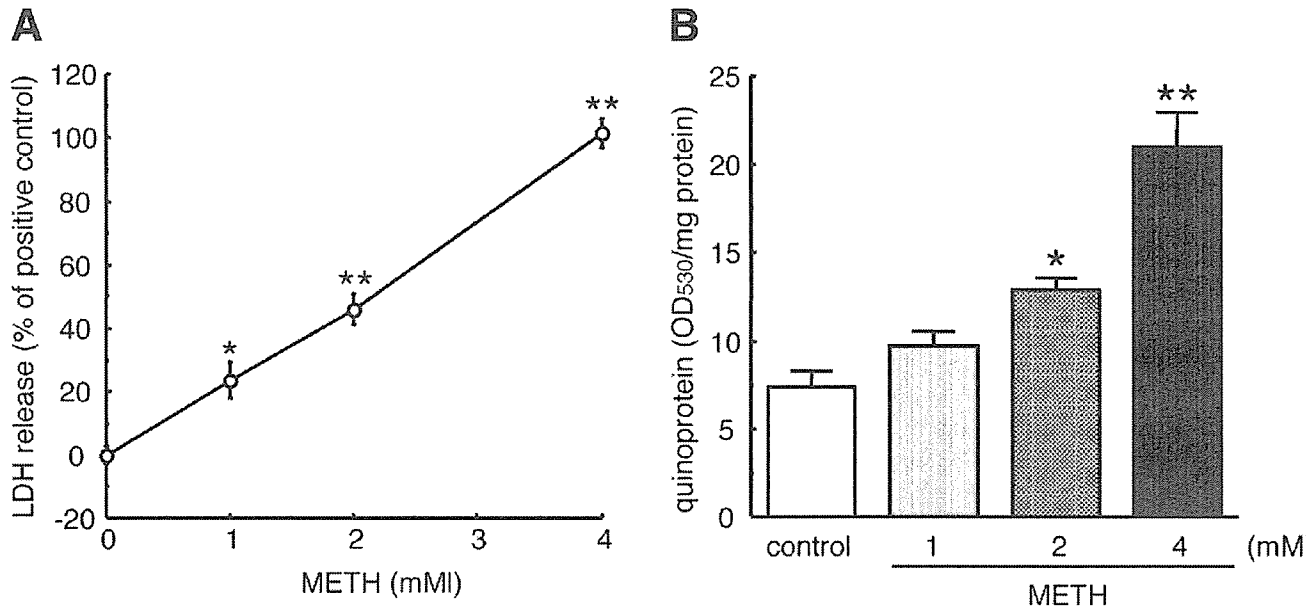

Figure 1. METH-induced neurotoxicity and quinoprotein formation in CATH.a cells. LDH release from CATH.a cells after 24 h exposure to various concentrations of METH (***A***). Each value of released LDH is expressed as the mean ± SEM in percentage of Tween-20-treated positive control in six experiments. **P*<0.01, ***P*<0.001 vs. control group without METH. Quinoprotein formation in CATH.a cells after 24-h exposure to various concentrations of METH (***B***). Each value is expressed as the mean ± SEM of OD530/mg protein in 6–8 experiments. **P*<0.05, ***P*<0.001 vs. control group without METH.

Fig. 2

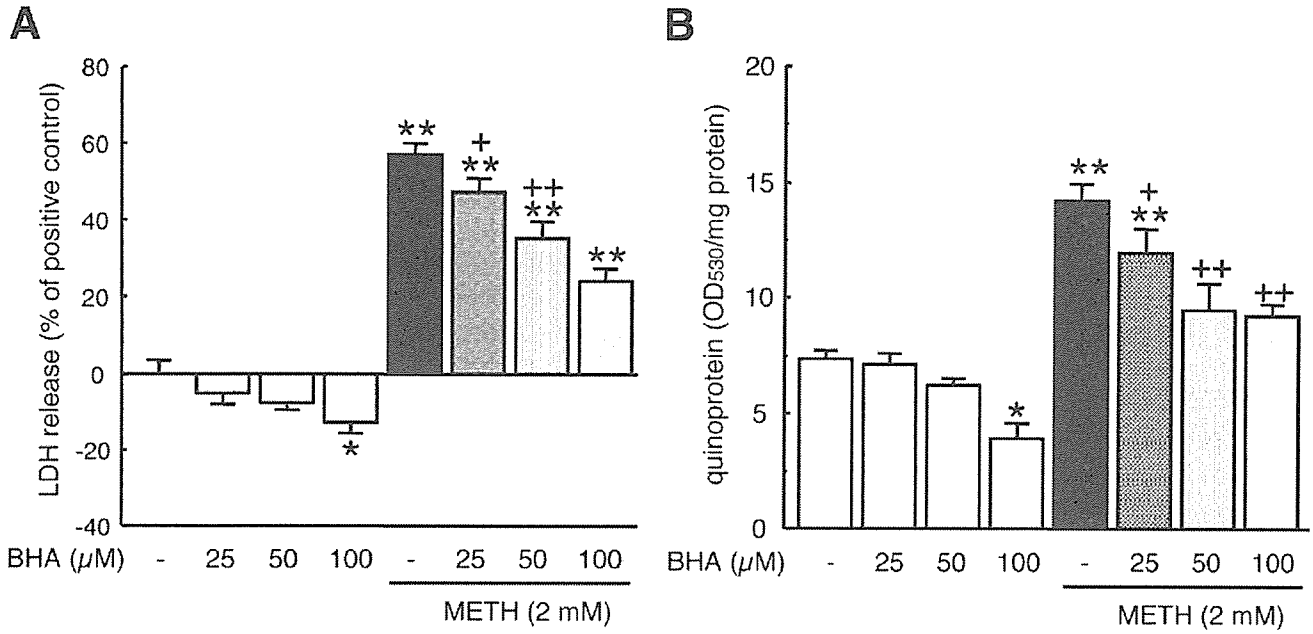

Figure 2. Effects of quinone reductase inducer on METH-induced neurotoxicity and quinoprotein formation in CATH.a cells. Effects of BHA on METH-induced neurotoxicity (***A***).CATH.a cells were pretreated with 25–100 μM BHA for 6 h and subsequently cotreated with 2 mM METH for 24 h. Each value of released LDH is expressed as the mean ± SEM in percentage of Tween-20-treated positive control (n=6). *P<0.05, **P<0.001 vs. untreated control group, +P<0.05, ++P<0.001 vs. METH-treated group. Effects of BHA on METH-induced quinoprotein formation (***B***). CATH.a cells were pretreated with 25–100 μM BHA for 6 h and subsequently cotreated with 2 mM METH for 24 h. Each value is expressed as the mean ± SEM of OD530/mg protein (n=6–8). *P<0.01, **P<0.001 vs. untreated control group, +P<0.05, ++P<0.001 vs. METH-treated group.

Fig. 3

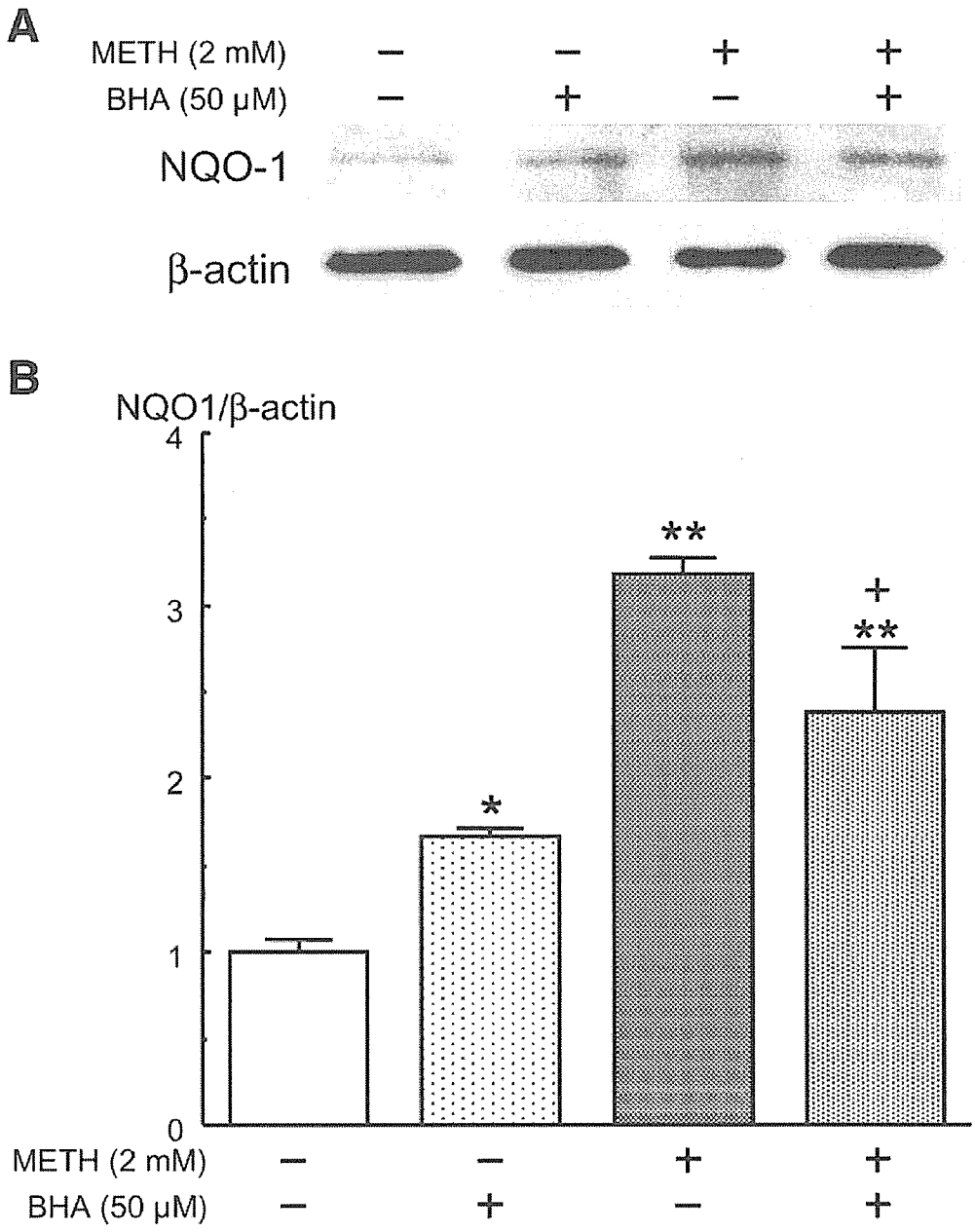

Figure 3. Effects of BHA and METH on NQO-1 expression in CATH.a cells. Western blot analysis of NQO-1 and β-actin (***A***). CATH.a cells were pretreated with 50 μM BHA for 6 h and subsequently cotreated with 2 mM METH for 24 h. Semiquantitative analysis of the NQO-1 expression in CATH.a cells (***B***). Each value is expressed as the mean ± SEM of the ratio for intensities of the band corresponding to NQO-1 and β-actin (n=4–5). *$P < 0.05$, **$P < 0.001$ vs. untreated control group. +$P < 0.05$ vs. METH-treated group.

Fig. 4

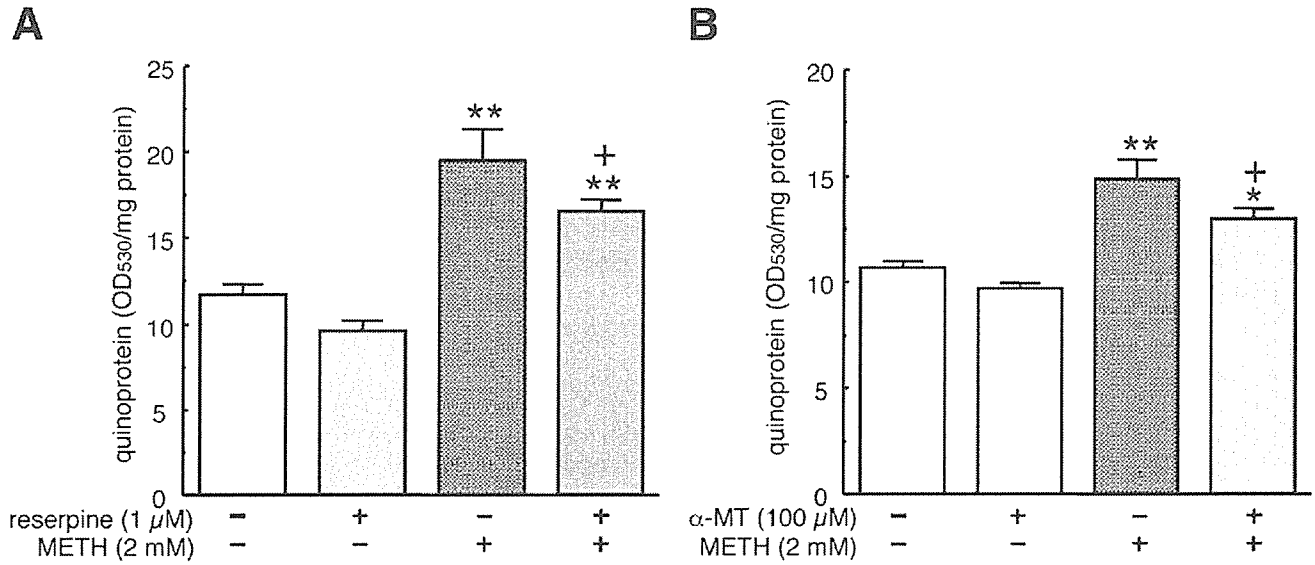

Figure 4. Effects of DA depletion on METH-induced quinoprotein formation in CATH.a cells. CATH.a cells were pretreated with 1 μM reserpine (***A***) or 100 μM α-MT (***B***) for 24 h and subsequently cotreated with 2 mM METH for 24 h. Each value is expressed as the mean ± SEM of OD530/mg protein in 6–8 experiments. **P*<0.05, ***P*<0.001 vs. untreated control group, +*P*<0.05 vs. METH-treated group.

Fig. 5

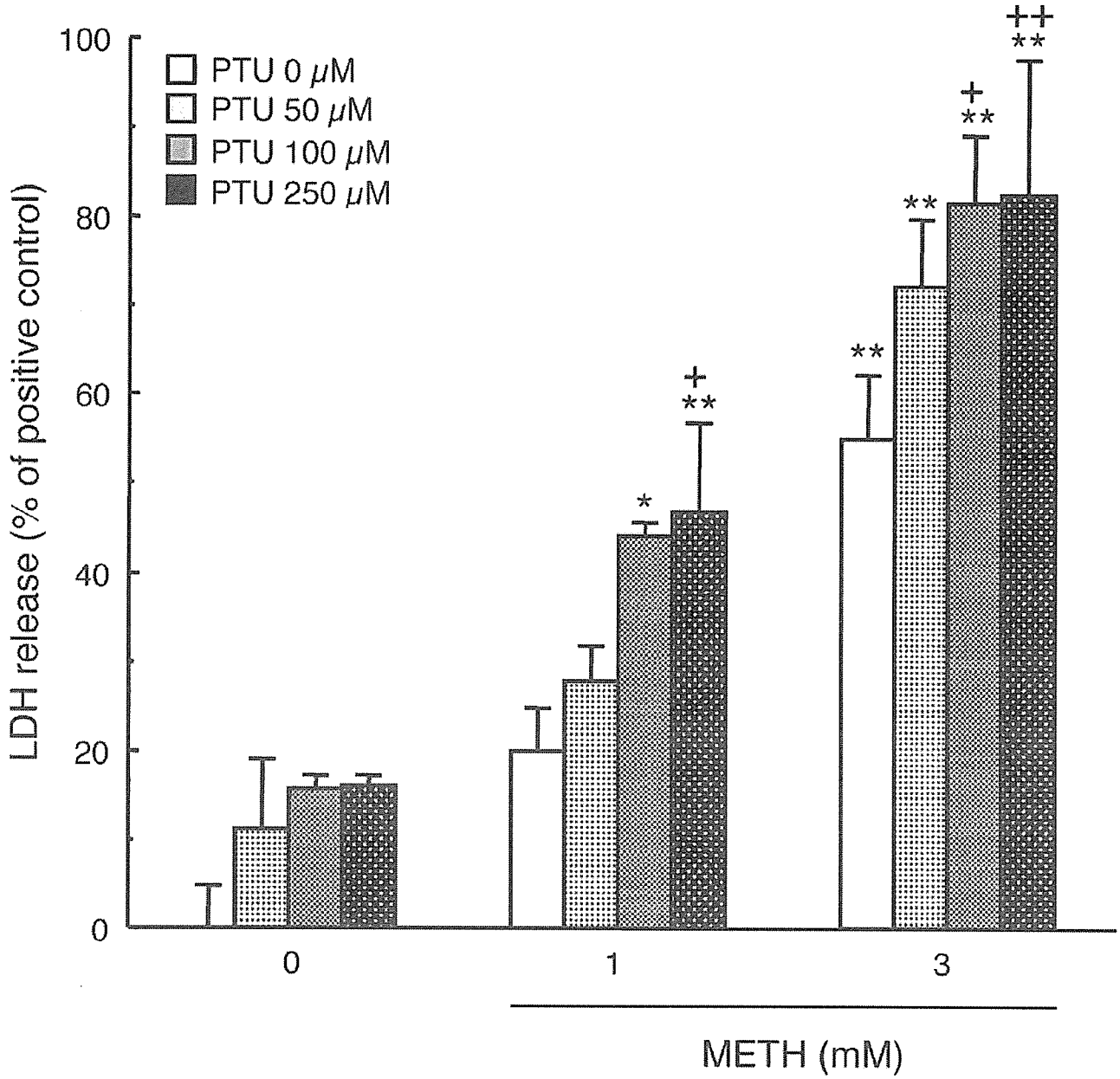

Figure 5. Effects of tyrosinase inhibitor on METH-induced neurotoxicity in CATH.a cells. CATH.a cells were treated with PTU (50–250 μM) and/or various concentration of METH for 24 h. Each value of released LDH is expressed as the mean ± SEM in the percentage of Tween 20-treated positive controls (n=4). *P<0.05, **P<0.001 vs. each control group without METH, +P<0.05, ++P<0.01 vs. METH dose-matched controls without PTU.

Fig. 6

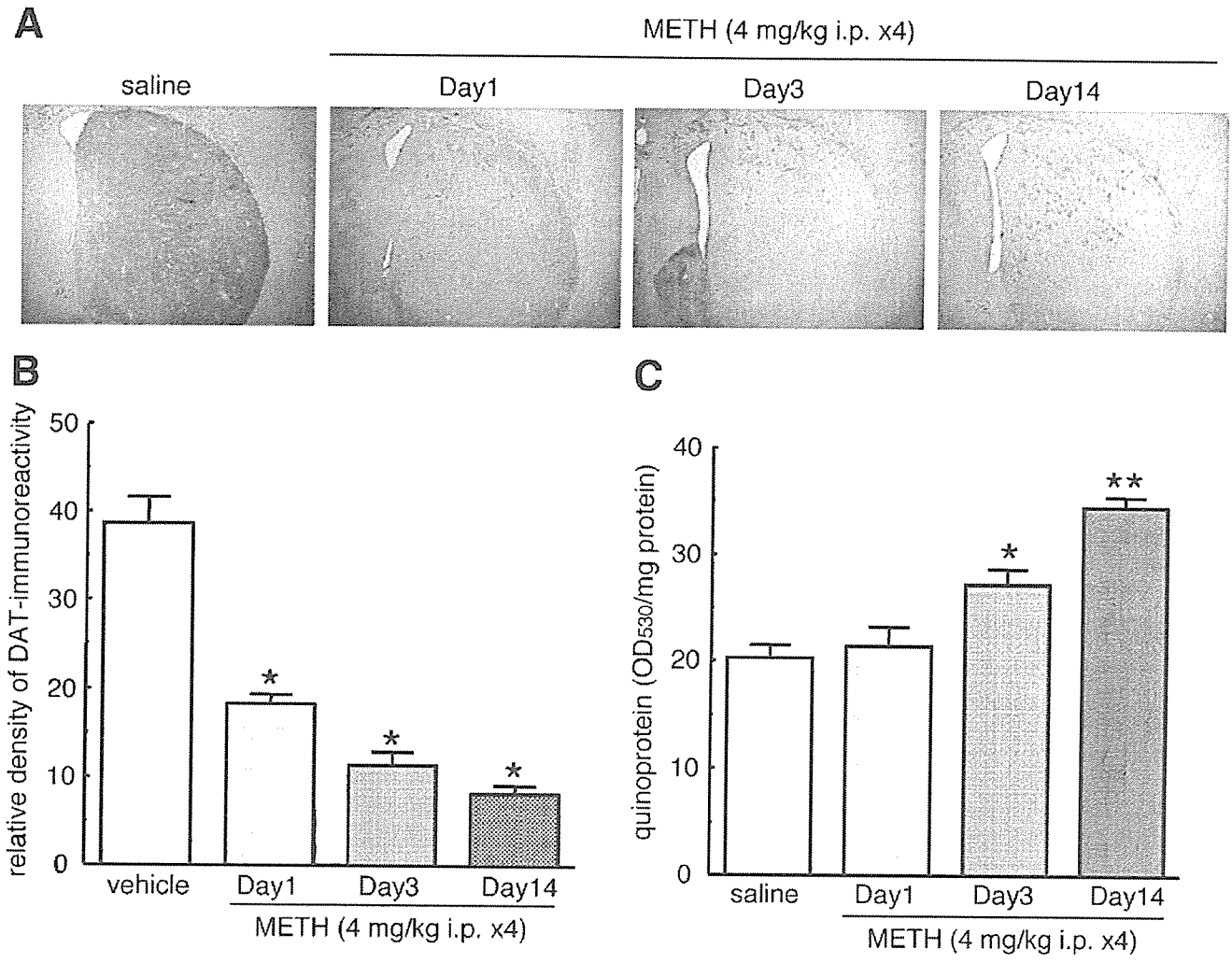

Figure 6. METH-induced neurotoxicity and quinoprotein formation in the striatum of BALB/c mice. Reduction of DAT in the striatum of BALB/c mice injected with METH. Representative photomicrographs of DAT-immunoreactive signals in the striatum of mice 1, 3, and 14 days after repeated METH injections (4 mg/kg×4, ip with 2 h interval) (*A*). Quantitative data of the relative density of DAT-positive signals in the striatum of mice 1, 3, and 14 days after repeated METH injections (***B***). Each value is expressed as the mean ± SEM of optical density of 6–8 animals per group. **P*<0.001 vs. vehicle-injected control mice. Quinoprotein formation in the striatum of BALB/c mice 1, 3, and 14 days after repeated METH injections (***C***). Each value is expressed as the mean ± SEM of OD530/mg protein of 6–8 animals per group. **P*<0.01, ***P*<0.001 vs. vehicle-injected control mice.

Fig. 7

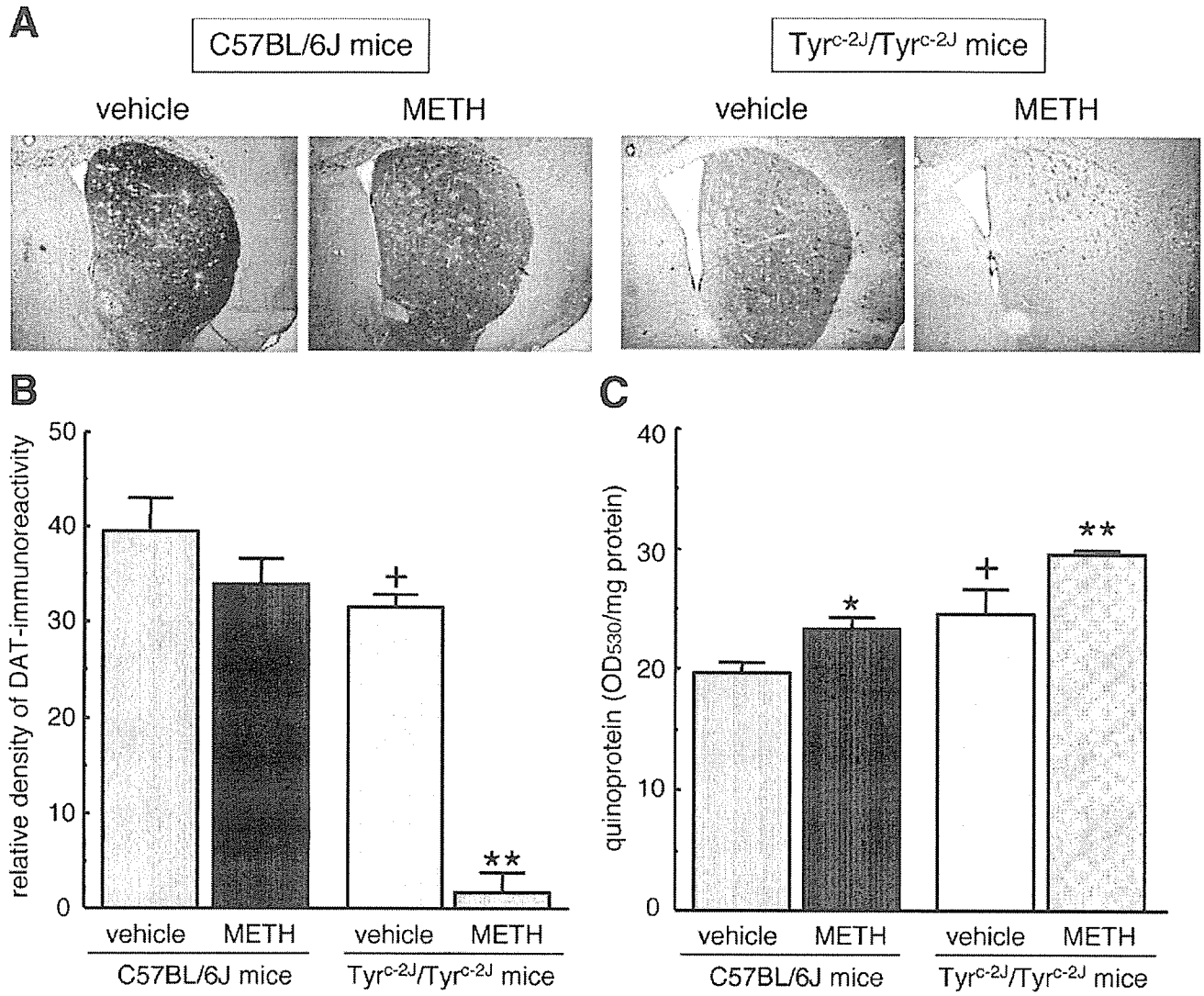

Figure 7. Effects of tyrosinase on METH-induced reduction of DAT and quinoprotein formation in the striatum of C57BL/6J and tyrosinase null mice injected with METH. Representative photomicrographs of DAT-immunoreactive signals in the striatum of C57BL/6j mice or tyrosinase null $Tyr^{c\text{-}2J}/Tyr^{c\text{-}2J}$ mice 3 days after repeated METH injections (4 mg/kg×4, ip with 2 h interval) (***A***). Quantitative data of the relative density of DAT-positive signals in the striatum of C57BL/6J mice or $Tyr^{c\text{-}2J}/Tyr^{c\text{-}2J}$ mice 3 days after repeated METH injections (***B***). Each value is expressed as the mean ± SEM in the percentage of vehicle-injected each control animals (n=6–8 mice per group). $^{**}P<0.001$ vs. vehicle-injected each control mice, $+P< 0.05$ vs. vehicle-injected C57BL/6j mice. Quinoprotein formation in the striatum of C57BL/6J mice or $Tyr^{c\text{-}2J}/Tyr^{c\text{-}2J}$ mice 3 days after repeated METH injections (***C***). Each value is expressed as the mean ± SEM of OD530/mg protein of 6–8 animals per group. $^{*}P<0.05$, $^{**}P<0.01$ vs. vehicle-injected each control mice, $+P < 0.05$ vs. vehicle-injected C57BL/6J mice.

Fig. 8

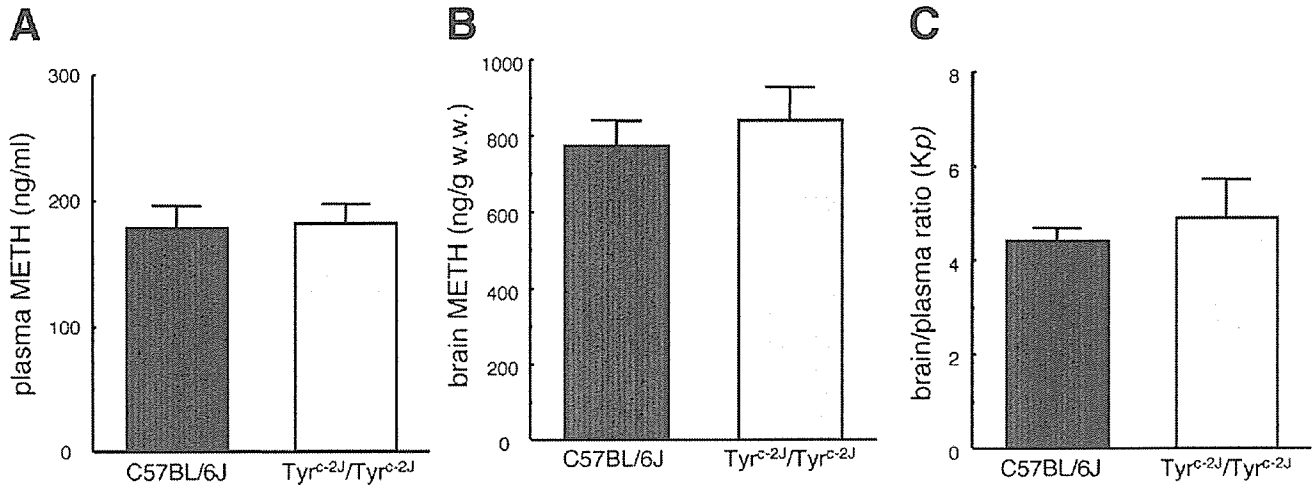

Figure 8. METH concentration in plasma (***A***) and brain (***B***) and the brain/plasma ratio (K*p*) (***C***) of C57BL/6J mice and tyrosinase null Tyr^{c-2J}/Tyr^{c-2J} mice 2 h after METH injection (4 mg/kg×1, ip). Each value is expressed as the mean ± SEM of 5–6 animals per group.

Fig. 9

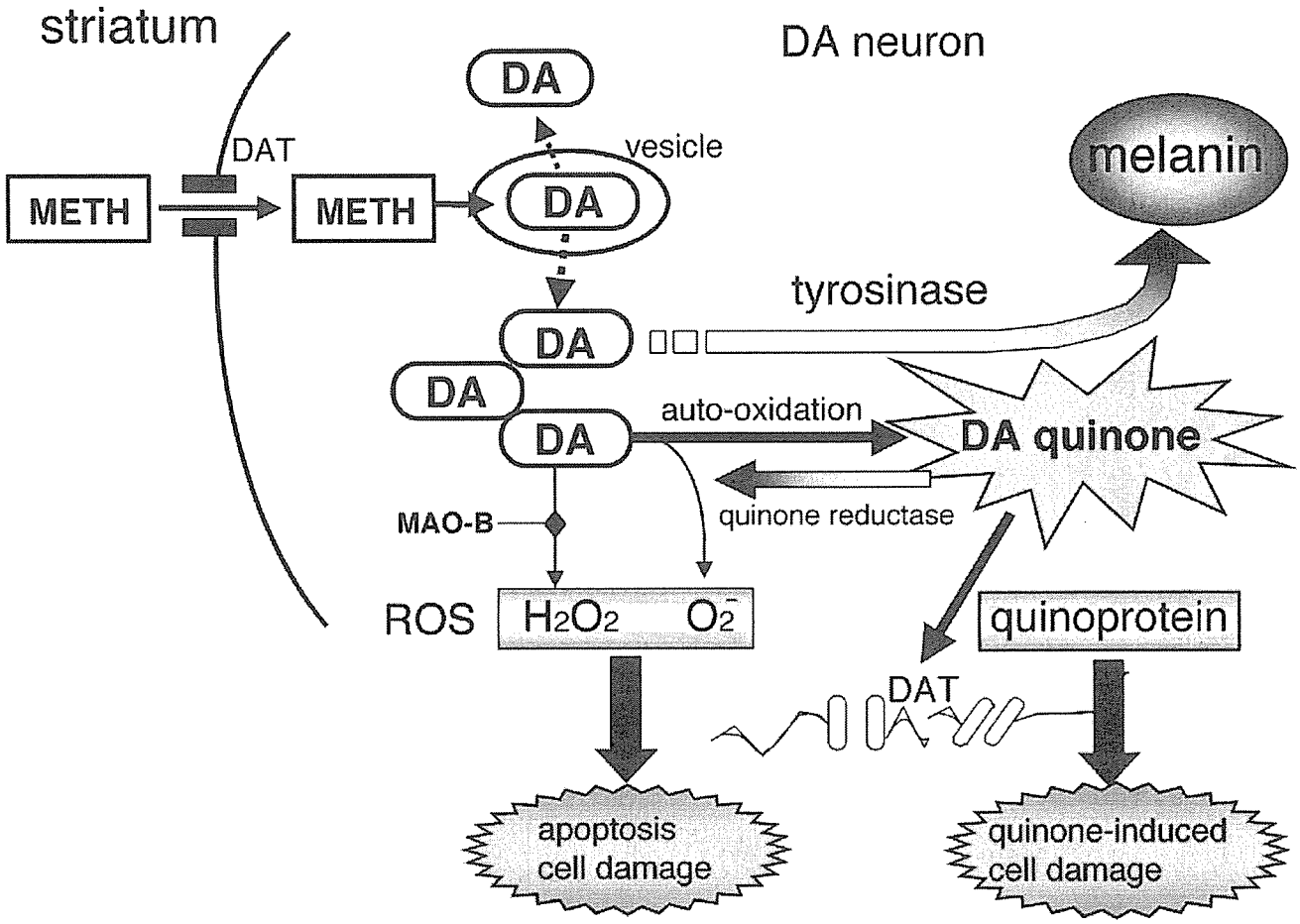

Figure 9. Schematic diagram showing involvement of DA quinone formation in METH-induced dopaminergic neurotoxicity and protective effects of quinone reductase and tyrosinase.

平成 17 年度厚生労働科学研究費補助金
（厚生労働科学特別研究事業）

脱法ドラッグの構造修飾特性とその依存性および神経毒性発現の関連性

課題番号：H17-特別-033

研究報告書

主任研究者：舩田正彦
（国立精神・神経センター　精神保健研究所）

2006 年 3 月 30 日　発行